

# SEMI-SMOOTH NEWTON METHODS FOR NONLINEAR COMPLEMENTARITY FORMULATION OF COMPOSITIONAL TWO-PHASE FLOW IN POROUS MEDIA \*

QUAN M. BUI<sup>†</sup> AND HOWARD C. ELMAN<sup>‡</sup>

**Abstract.** Simulating compositional multiphase flow in porous media is a challenging task, especially when phase transition is taken into account. The main problem with phase transition stems from the inconsistency of the primary variables such as phase pressure and phase saturation, i.e. they become ill-defined when a phase appears or disappears. Recently, a new approach for handling phase transition has been developed, whereby the system is formulated as a nonlinear complementarity problem (NCP). Unlike the widely used primary variable switching (PVS) method which requires a drastic reduction of the time step size when a phase appears or disappears, this approach is more robust and allows for larger time steps. One way to solve an NCP system is to reformulate the inequality constraints as a non-smooth equation using a complementary function (C-function). Because of the non-smoothness of the constraint equations, a semi-smooth Newton method needs to be developed. In this work, we consider two methods for solving NCP systems used to model multiphase flow: (1) a semi-smooth Newton method for two C-functions: the minimum and the Fischer-Burmeister functions, and (2) a new inexact Newton method based on the Jacobian smoothing method for a smooth version of the Fischer-Burmeister function. We show that the new method is robust and efficient for standard benchmark problems as well as for realistic examples with highly heterogeneous media such as the SPE10 benchmark.

**Key words.** semi-smooth Newton, two-phase flow, nonlinear complementarity problem, phase transition, porous media.

**1. Introduction.** Multiphase flow is a critical process in a wide range of hydrodynamic phenomena, including carbon sequestration, reservoir simulation, and groundwater remediation. For simulation, it would be ideal to have a complete knowledge of the state and composition of the fluid phases in the flow. However, this is not an easy task given the complex physics involved. Some of the most important effects that need to be taken into consideration include capillarity, miscibility, and especially phase transitions. If not handled correctly, these effects can introduce nonphysical numerical oscillations in computational solutions of the strongly nonlinear system of partial differential equations.

Phase transitions have posed a major challenge for multiphase, multi-component models since the 1980s. If not handled correctly, they can cause numerical oscillations in solutions of these models, making such solutions physically inconsistent and unusable. There have been many attempts to address the problems with phase transitions and determine the correct local thermodynamic state for compositional multiphase flow. In general, most of these can be classified into two common classes of methods: flash calculation [2, 16, 17, 21, 34, 43] and primary variables switching (PVS) [26, 41]. Flash calculation computes the local thermodynamic state from the overall mass of the individual components. While this method is stable with regard to determining the thermodynamic state, it tends to be inefficient because it requires solution of a large nonlinear system of equations at each time step (in addition to solution of the linearized systems) to recover all the thermodynamic quantities of interest. The second class, PVS, involves adapting the primary variables to the thermodynamic constraints locally. The idea is that whenever phase transitions occur, physical variables that are physically inconsistent (indicated by negative saturation, for example) are switched to well-defined quantities. The governing equations related to those variables are also modified accordingly. Although this approach is locally more efficient than flash calculations, it suffers from irregular convergence behavior in the nonlinear solve, which is typically addressed by substantial reduction in time step size [20]. This feature is not desirable for simulations over a long period of time, usually encountered in groundwater remediation or transport of nuclides in a nuclear waste repository. In addition to flash calculations and PVS, there are other formulations to handle phase transitions such as negative saturation [1], and introduction of persistent primary variables [9, 33, 35].

Recently, a new approach has been developed for handling the phase transitions by formulating the system of equations as a nonlinear complementarity problem (NCP) [8, 30, 32]. In contrast to PVS, NCP has the advantage that the set of primary variables is consistent throughout the simulation, and no primary variable switching is needed. NCP requires a complementary function, referred to as a C-function, employed

\*This work is funded by the U. S. Department of Energy Office of Advanced Scientific Computing Research, Applied Mathematics program, under Award Number DE-SC0009301.

<sup>†</sup>Corresponding author. Applied Math, Stats, and Scientific Computation, University of Maryland, College Park, MD (mquanbui@math.umd.edu).

<sup>‡</sup>Department of Computer Science and Institute for Advanced Computer Studies, University of Maryland, College Park, MD (elman@cs.umd.edu).

to rewrite the inequality constraints for the thermodynamic state as a non-smooth equation, which requires a *semi-smooth* Newton method [3, 37, 38] to solve. Most of the previous work in multiphase flow using the NCP approach employs the minimum function as the C-function due to its simplicity for implementation and the fact that it is piecewise linear with respect to the arguments. Even though the semi-smooth Newton method applied to the NCP using the minimum function as a C-function is observed to have quadratic convergence for simple problems in porous media (see [8]), we find that it exhibits poor convergence and even diverges for standard benchmark problems, as well as examples considered in this work. An alternative to the minimum function is the Fischer-Burmeister function, which has recently been employed as the C-function for NCP formulation of incompressible two-phase flow in [42]. As we will show, this choice of C-function can help mitigate the lack of robustness observed in using the Newton-min algorithm for NCP formulation of compositional two-phase flow with phase transitions. We then draw on this experience and develop a new method for the nonlinear solve based on a smooth version of the Fischer-Burmeister function. Our method can be considered a variant of the Jacobian smoothing method summarized in [25]. Compared to the non-smooth approaches that use the minimum and the Fischer-Burmeister functions, our new method is more robust and efficient for problems with highly heterogeneous media, and it also scales optimally with problem size.

We consider a two-phase, two-component system with phase transitions as our model problem. We describe this model in detail in section 2, and in section 3, we describe the NCP formulation for it. We briefly review the semi-smooth Newton framework and introduce our new algorithm in section 4. In section 5, several numerical tests are presented that demonstrate the robustness and scalability of the new algorithm. Some concluding remarks as well as future work are presented in section 6.

## 2. Problem Statement.

**2.1. Governing Equations.** In this work, we consider a simplified two-phase two-component model with phase transitions. The phases consist of liquid and gas, and the components are water and hydrogen. We also make the following assumptions: (1) water does not vaporize so the gas phase contains only hydrogen, and (2) the amount of hydrogen dissolved in the liquid phase is small. For the two components, the mass conservation equations read

$$(1) \quad \phi \frac{\partial(\rho_l^w S_l)}{\partial t} + \nabla \cdot (\rho_l^w \mathbf{q}_l - j_l^h) = 0,$$

$$(2) \quad \phi \frac{\partial(\rho_l^h S_l + \rho_g^h S_g)}{\partial t} + \nabla \cdot (\rho_l^h \mathbf{q}_l + \rho_g^h \mathbf{q}_g + j_l^h) = 0,$$

where the subscripts  $l, g$  denote the liquid and gas phases, and the superscripts  $w, h$  denote the water and hydrogen components, respectively. The porosity of the medium is denoted  $\phi$ ,  $S_\alpha, \mathbf{q}_\alpha$  are the saturation and velocity of phase  $\alpha$ , respectively;  $\rho_l^h$  is the dissolved hydrogen mass concentration in the liquid phase; and  $j_l^h$  is the diffusion flux of hydrogen in the liquid phase. The Darcy velocity  $\mathbf{q}_\alpha$  follows the Darcy-Muskat law

$$(3) \quad \mathbf{q}_\alpha = -\mathbf{K} \lambda_\alpha \nabla(P_\alpha - \rho_\alpha \mathbf{g}), \quad \alpha = l, g,$$

where  $\mathbf{K}$  is the absolute permeability,  $\lambda_\alpha, P_\alpha$ , and  $\rho_\alpha$  are the mobility, pressure, and density of phase  $\alpha$ , and  $\mathbf{g}$  is the gravitational acceleration. The mobility  $\lambda_\alpha$  of phase  $\alpha$  is defined as the ratio between the phase relative permeability  $k_{r\alpha}$  and the phase viscosity  $\mu_\alpha$ :  $\lambda_\alpha = k_{r\alpha}/\mu_\alpha$ . Using Fick's law, the diffusion flux of hydrogen in liquid  $j_l^h$  in (1) and (2) can be expressed as

$$(4) \quad j_l^h = -\phi S_l D_l^h \nabla \rho_l^h,$$

where  $D_l^h$  is the hydrogen molecular diffusion coefficient in liquid. Since we assume incompressibility of the liquid phase, the mass density of the water component in the liquid phase is constant, i.e.  $\rho_l^w = \rho_w^{std}$ . To capture capillarity effects, the jump in the pressure at the interface of the two phases is modeled by the relation

$$(5) \quad P_g = P_l + P_c(S_l)$$

where  $P_c$  is the capillary pressure. Additionally, we have the constraints

$$(6) \quad S_l + S_g = 1.$$

To close the model, we also need a set of equations for the thermodynamic equilibrium when the gas phase is present, i.e. how much hydrogen can dissolve into the liquid phase at a certain pressure. Assuming low solubility of hydrogen in the liquid phase, Henry's law can be used to connect the gas pressure  $P_g$  and the dissolved hydrogen mass concentration in liquid  $\rho_l^h$ :

$$(7) \quad \rho_l^h = C_h P_g,$$

where  $C_h = HM^h = \rho_w^{std} M^h / (M^w K^h)$ ,  $H$  is the Henry's law constant,  $K^h$  is a constant specific to the mixture, and  $M^i$ ,  $i \in \{w, h\}$ , is the molar mass of the  $i$ -th component. Since we neglect water vapor, we can apply the ideal gas law for the gas phase. This leads to the relation

$$(8) \quad \rho_g^h = \rho_g = C_v P_g,$$

where  $C_v$  is a constant and  $C_v = M^h / (RT)$ ;  $T$  is the temperature and  $R$  the ideal gas constant.

**2.2. Relative Permeabilities and Capillary Pressure.** We employ the nonlinear Van Genuchten [40] model for relative permeabilities and capillary pressure:

$$(9) \quad k_{rl} = \sqrt{S_{le}} \left(1 - (1 - S_{le}^{1/m})^m\right)^2, \quad k_{rg} = \sqrt{1 - S_{le}} \left(1 - S_{le}^{1/m}\right)^{2m},$$

$$(10) \quad P_c = P_r \left(S_{le}^{-1/m} - 1\right)^{1/n},$$

$$(11) \quad S_{le} = \frac{1 - S_l}{1 - S_{lr} - S_{gr}}, \quad m = 1 - \frac{1}{n},$$

where  $P_r$  is the entry pressure. Notice that the function  $P_c(S_l)$  in the Van Genuchten model is only defined for  $S_l \in [S_{lr}, 1 - S_{gr}]$  and  $P'_c$  is unbounded near  $S_{lr}$  and  $1 - S_{gr}$ . Thus, it is necessary to modify the model to limit the growth of  $P'_c$  and extend it for  $S_l \in \mathbb{R}$ , since the value of  $S_l$  can become larger than  $1 - S_{gr}$  or less than  $S_{lr}$  during the nonlinear iteration. We use the following regularization as presented in [32] with parameter  $\epsilon = 10^{-5}$ : In this regularization, for the saturation that is outside of the domain, capillary pressure is computed by a linear extrapolation from the regularization points  $S_{lr} + \mathcal{O}(\epsilon)$  and  $1 - S_{gr} - \mathcal{O}(\epsilon)$  with the slopes  $P'_c(S_{lr} + \mathcal{O}(\epsilon))$  and  $P'_c(1 - S_{gr} - \mathcal{O}(\epsilon))$ , respectively.

**2.3. Primary Variables.** There are many ways to choose a set of primary variables, depending on the problem formulation and applications. In our model example, a convenient choice is the liquid pressure, liquid saturation, and the concentration of hydrogen in the liquid phase. We then have our solution vector  $u = \{P_l, S_l, \rho_l^h\}$ . Unlike in other methods such as primary variable switching, for NCP, the choice of primary variables is fixed throughout the simulation.

**3. Nonlinear Complementarity Problem.** In its simplest form, a nonlinear complementarity problem with respect to a smooth function  $f : \mathbb{R}^N \mapsto \mathbb{R}^N$  is to find a vector  $u \in \mathbb{R}^N$  such that

$$(12) \quad u \geq 0, \quad f(u) \geq 0, \quad u^T f(u) = 0,$$

A slightly more general form of the last equation in (12) reads

$$(13) \quad g(u)^T f(u) = 0,$$

where  $g : \mathbb{R}^N \rightarrow \mathbb{R}^N$  is another smooth function. As we have mentioned in section 2, for the solution of (1) and (2) to be valid, the pressure, saturation, and hydrogen concentration in the liquid phase must satisfy the constraints in (6) and (7). These conditions can be reformulated as an NCP as follows:

$$(14) \quad 1 - S_l \geq 0, \quad C_h P_g - \rho_l^h \geq 0, \quad (1 - S_l)(C_h P_g - \rho_l^h) = 0,$$

where  $u = (P_l \ S_l \ \rho_l^h)^T$ , and the functions in (13) are  $g(u) = 1 - S_l$ ,  $f(u) = C_h P_g - \rho_l^h$ . A very popular approach to solve (14) is to transform it into a semi-smooth nonlinear equation via a complementarity function (also called C-function)  $\Phi(a, b) : \mathbb{R}^2 \rightarrow \mathbb{R}$ , which satisfies

$$(15) \quad \Phi(a, b) = 0 \iff a \geq 0, \quad b \geq 0, \quad ab = 0.$$

We can extend the definition of  $\Phi$  (15) from  $\mathbb{R}^2$  to  $\mathbb{R}^N$ , where  $N$  is also the number of elements in the mesh, by applying it (15) componentwise to  $1 - S_l$  and  $C_h P_g - \rho_l^h$  and obtain the nonlinear system

$$(16) \quad \Theta(u) = \begin{pmatrix} \Phi(1 - (S_l)_1, (C_h P_g - \rho_l^h)_1) \\ \Phi(1 - (S_l)_2, (C_h P_g - \rho_l^h)_2) \\ \dots \\ \Phi(1 - (S_l)_N, (C_h P_g - \rho_l^h)_N) \end{pmatrix}.$$

Then, solving the NCP problem in (14) is equivalent to solving  $\Theta(u) = 0$ . As discussed in the next section, combining this complementarity condition with the discrete PDEs enables use of a nonlinear solution algorithm that automatically enforces the constraints (6)-(7). There are many examples of C-functions [25]. In this work, we focus on two popular choices

$$(17) \quad \Phi_{\min}(a, b) = \min(a, b)$$

$$(18) \quad \Phi_{FB}(a, b) = \sqrt{a^2 + b^2} - (a + b) \quad (\text{Fischer-Burmeister})$$

The minimum function is convenient because it is piecewise linear with respect to the variables  $a$  and  $b$ , which simplifies the computation of the Jacobian in each nonlinear iteration [30]. When the gas phase is not present, (17) reduces to  $1 - S_l = 0$ . When the gas phase appears,  $1 - S_l > 0$  and the constraint equation is governed by Henry's law (7). Recently, the Fischer-Burmeister function has been shown to have good performance for the case of incompressible two-phase flow [42].

Although we do not employ any line search strategy in this work, we note that compared to the Fischer-Burmeister function, the minimum function is less useful with respect to globalization with line search strategies [25]. As shown and discussed in [5, 6, 7], global semi-smooth Newton methods may diverge even for linear C-functions if the starting point is not close enough to a solution. In global semi-smooth Newton approaches, this can be handled using line search, in which a *merit function* is used to enhance robustness by evaluating the quality of new iterates. In this scenario, it is desirable for the natural merit function  $\Psi = \|\Phi\|^2$  to be smooth because the search direction at each nonlinear iteration is usually chosen based on the derivative of  $\Psi$  [29]. The merit function associated with the minimum function  $\Psi_{\min} = \|\Phi_{\min}(a, b)\|^2$ , however, does not satisfy this condition. In contrast, the Fischer-Burmeister merit function  $\Psi_{FB} = \|\Phi_{FB}(a, b)\|^2$  is continuously differentiable as observed in [24].

**4. Solution Algorithm.** We consider solving the coupled system consisting of (1), (2), and (14) fully implicitly. We use a cell-centered finite volume method for spatial discretization, as it is a natural way to preserve the mass conservation property of the balance (1) and (2). In addition, it can deal with the case of discontinuous permeability coefficients, and it is relatively straightforward to implement. For the time domain, we employ the backward Euler method to avoid a CFL stability restriction on the time step. Because this method is unconditionally stable, it also allows us to experiment with variable time stepping, which can significantly reduce execution time.

**4.1. Semi-smooth Newton Method.** We want to solve the system  $R(u) = 0$  where  $R(u)$  is the residual function given by

$$(19) \quad R(u) = \begin{cases} H(u) & (\text{from the PDEs}) \\ \Theta(u) & (\text{from the constraints}) \end{cases}$$

This is a system of  $3N$  equations and  $3N$  unknowns, where  $N$  is the number of elements in the mesh. A standard approach for solving nonlinear systems of equations is Newton's method, which requires solution of a linear system at each iteration  $k$ :

$$(20) \quad \left. \frac{\partial R}{\partial u} \right|_{u=u_k} \delta u = -R(u_k).$$

This method requires that the Jacobian  $\partial R/\partial u$  be defined everywhere. In the NCP formulation, the constraints  $\Theta$  are not differentiable when there is phase transition as the solution changes from satisfying  $1 - S_l = 0$  to  $C_h P_g - \rho_l^h = 0$ . To address this, we will consider a semi-smooth Newton method, which is

similar to Newton's method, except the derivative  $\Theta'$  is replaced by a member of the *subdifferential*  $\partial\Theta$  when  $\Theta$  is not differentiable. Let  $F : \mathbb{R}^n \mapsto \mathbb{R}^n$  be a locally Lipschitz-continuous function and  $D_F$  be the set where  $F$  is differentiable; the B-subdifferential of  $F$  at  $x$  is defined as the set

$$\partial_B F(x) := \{G \in \mathbb{R}^{n \times n} : \exists x_k \in D_F \text{ with } x_k \rightarrow x, \nabla F(x_k) \rightarrow G\}.$$

Below is the algorithm for the general semi-smooth Newton method (see [25]).

---

**Algorithm 1** General semi-Smooth Newton method.

---

**while**  $k < \text{max\_iter}$  and  $\text{res} > \text{tol}$  **do**

- (1) Given  $u^0$ ,  $k = 0$
- (2) Select an element  $J_k \in \partial_B \Theta(u^k)$
- (3) Solve the system

$$\begin{pmatrix} H'(u^k) \\ J_k(u^k) \end{pmatrix} \Delta u^k = \begin{pmatrix} -H(u^k) \\ -\Theta(u^k) \end{pmatrix}$$

- (4) Update  $u^{k+1}$ :  $u^{k+1} = u^k + \Delta u^k$
- 

To compute  $J_k$  in the algorithm above, one can use an active set strategy [27]. For multiphase flow with phase appearance and disappearance, the idea is to define the set of indices for the cells in which the gas phase is present (see [8, 30]). Let  $A^k := \{j : 1 - (S_l)_j \geq (C_h P_g - \rho_l^h)_j\}$ ,  $I^k := \{j : 1 - (S_l)_j < (C_h P_g - \rho_l^h)_j\}$ . Then for the minimum function, the  $j$ th row of  $J_k$  is equal to

$$(21) \quad \begin{cases} \frac{\partial}{\partial u} a(u)_j & \text{if } j \in I^k \\ \frac{\partial}{\partial u} b(u)_j & \text{if } j \in A^k \end{cases}$$

where  $a(u)_j = 1 - (S_l)_j$  and  $b(u)_j = (C_h P_g - \rho_l^h)_j$ . For the Fischer-Burmeister function, we can compute the  $j$ th row of  $J_k$  as follows:

$$(22) \quad \begin{cases} \frac{1}{\sqrt{a(u)_j^2 + b(u)_j^2}} \left( a(u)_j \frac{\partial}{\partial u} a(u)_j + b(u)_j \frac{\partial}{\partial u} b(u)_j \right) - \left( \frac{\partial}{\partial u} a(u)_j + \frac{\partial}{\partial u} b(u)_j \right) & \text{if } a(u)_j^2 + b(u)_j^2 \neq 0 \\ (\alpha_i - 1) \frac{\partial}{\partial u} a(u)_j + (\beta_i - 1) \frac{\partial}{\partial u} b(u)_j & \text{otherwise} \end{cases}$$

where for all  $i$  such that  $a(u)_j^2 + b(u)_j^2 = 0$ ,  $\alpha_i$  and  $\beta_i$  are arbitrary nonnegative constants satisfying  $\alpha_i^2 + \beta_i^2 = 1$ . For a more complete treatment of semi-smooth Newton methods, we refer to [25].

**4.2. Jacobian Smoothing Method.** An alternative to the semi-smooth approach is to employ a smooth approximation to the non-smooth function  $\Theta$ . The idea was originally developed in the context of variational inequalities [14, 15] and generalized to more general nonlinearities and infinite dimensions in [13]. Let  $G : \mathbb{R}^n \times \mathbb{R}_+ \mapsto \mathbb{R}^n$  such that for any  $\tau > 0$ ,  $G(\cdot, \tau)$  is continuously differentiable on  $\mathbb{R}^n$  and

$$(23) \quad \|\Theta(u) - G(u, \tau)\| \rightarrow 0, \quad \text{as } \tau \rightarrow 0.$$

Then, given a sequence  $\tau^k$ ,  $k = 0, 1, 2, \dots$ , we can solve the system in (19) inexactly using  $G'(u^k, \tau^k)$  as an approximation to the generalized Jacobian  $J_k = \partial_B \Theta(u^k)$ . In this work, we explore a smooth approximation to the Fischer-Burmeister functions given by

$$(24) \quad G_{FB}(u, \tau) = \sqrt{a^2 + b^2 + 2\tau} - (a + b)$$

The complete algorithm is as follows:

**Algorithm 2** Jacobian Smoothing Method.

---

**while**  $k < \text{max\_iter}$  and  $\text{res} > \text{tol}$  **do**
(1) Given  $u^0$ ,  $k = 0$ , and  $\tau^0$ 

(2) Solve the system

$$\begin{pmatrix} H'(u^k) \\ G'(u^k, \tau^k) \end{pmatrix} \Delta u^k = \begin{pmatrix} -H(u^k) \\ -\Theta(u^k) \end{pmatrix}$$

(3) Update the smoothing parameter  $\tau$ 

$$\tau^{k+1} = \beta \tau^k \text{ for } \beta \in (0, 1)$$

(4) Update  $u^{k+1}$ 

$$u^{k+1} = u^k + \Delta u^k$$


---

There also exist smooth approximations to the minimum function. In particular, we experimented with the Chen-Harker-Kanzow-Smale smoothing [12, 28],

$$(25) \quad G_{\min}(u, \tau) = (a + b) - \sqrt{(a - b)^2 + 4\tau}.$$

However, in our experience, this smooth version of the minimum function does not improve the convergence of the semi-smooth Newton's method significantly, and we do not include the results here.

**4.3. Linear System.** Assuming that each physical variable is ordered lexicographically, each step of the nonlinear iteration (step 3 in Algorithm 1 and step 2 in Algorithm 2) requires solution of a large sparse, non-symmetric, indefinite linear system of the form

$$(26) \quad \begin{pmatrix} A_{11} & A_{12} & A_{13} \\ A_{21} & A_{22} & A_{23} \\ A_{31} & A_{32} & A_{33} \end{pmatrix} \begin{pmatrix} u_1 \\ u_2 \\ u_3 \end{pmatrix} = \begin{pmatrix} f_1 \\ f_2 \\ f_3 \end{pmatrix}.$$

where  $u_1, u_2, u_3$  are the corrections to  $S_l, P_l, \rho_l^h$ , respectively. The matrices in the first two rows are the discretized version of the linearized operators from the PDEs, and the last row corresponds to the discrete derivative of the complementarity constraint equation introduced in (16). Iterative methods such as GMRES [39] are the only viable option to solve the system above, and preconditioning is critical for fast convergence. Here, all of our experiments use GMRES preconditioned with hypreMGR (see [11]), an AMG solver and preconditioner based on multigrid reduction and designed for systems of PDEs. Unlike ILU preconditioners in which one only needs to specify the level of fill (in  $\text{ILU}(k)$ ) or the threshold tolerance (in  $\text{ILU}(t)$ ), hypreMGR requires extra information regarding the block structure of the system and the order of reduction.

There exists a small but important difference in the structure of the matrices  $A$  created using the Jacobian smoothing method and the semi-smooth Newton methods. For the semi-smooth Newton methods with an active set strategy, the diagonal of the block  $A_{33}$  contains zeros for the cells that are devoid of the gas phase. In contrast, for  $\tau > 0$ , the diagonal of the block  $A_{33}$  is guaranteed to be nonzero for the Jacobian smoothing method regardless of the existence of phase transitions. Thus, the Jacobian smoothing method requires one fewer reduction step for hypreMGR, compared to semi-smooth Newton approaches, which leads to a decrease in both the number of GMRES iterations and execution time, as will become evident from the results presented in section 5.3.

**5. Numerical Results.** In this section, we describe the results of numerical experiments for solving the NCP systems using both the semi-smooth Newton's approach using the minimum and the Fischer-Burmeister functions, and the Jacobian smoothing method with the smooth Fischer-Burmeister function for the NCP formulation. All of these methods are implemented in Amanzi, a parallel open-source multi-physics C++ code developed as a part of the ASCEM project [4]. Although Amanzi was first designed for simulation of subsurface flow and reactive transport, its modular framework and concept of process kernels [22] allow new physics to be added relatively easily for other applications. The compositional two-phase flow simulator employed in this work is one such example. Amanzi works on a variety of platforms, from laptops to supercomputers. It also leverages several popular packages for mesh infrastructure and solvers through a unified input file. GMRES is also provided within Amanzi while hypreMGR is employed through HYPRE.

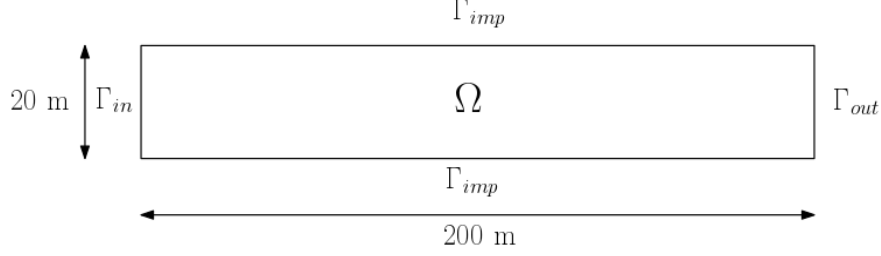


Fig. 1: Core domain for the gas infiltration example.

This section has three parts. In the first part, we show results using two benchmark problems that demonstrate the effectiveness of the NCP approach in handling phase appearance and disappearance. In the second part, we report the results for both two- and three-dimensional cases with highly heterogeneous media. In the last part, we perform a scalability study of the algorithms. Parallel test cases are run on Syrah, a Cray system with 5,184 Intel Xeon E5-2670 cores at the Lawrence Livermore National Laboratory Computing Center. Amanzi and other libraries are compiled with OpenMPI 1.6.5 and gcc-4.9.2.

For all the simulations presented here, the convergence tolerance for the nonlinear solve is  $\|F(x)\| \leq 10^{-6}$ , and the linear tolerance for GMRES is  $\|J\delta u_k - F(u_k)\| \leq 10^{-12}\|F(u_k)\|$ , which is the default in Amanzi. Depending on the performance of the nonlinear solver, a heuristic for choosing the time step is used: if the number of nonlinear steps (NS) required at a given time are less than 10, then the next time step  $dt_{next}$  is doubled,  $dt_{next} = 2 \cdot dt$ ; if  $NS \in [11, 15]$ , then the time step is kept fixed,  $dt_{next} = dt$ ; and if NS is greater than 15, then the time step is halved  $dt_{next} = dt/2$ . The maximum number of nonlinear iterations is  $max\_iter = 20$ .

**5.1. Benchmark problems.** These tests are derived from the MoMaS benchmark project [10], which is designed to evaluate the effectiveness of different approaches for handling gas phase appearance and disappearance. Pure hydrogen is injected into a two-dimensional homogeneous porous domain  $\Omega$ , which was initially 100% saturated with pure water. The domain is a rectangle of size 200m  $\times$  20m, and it is discretized only in the horizontal direction, leading to a quasi one-dimensional problem. There are three types of boundaries:  $\Gamma_{in}$  on the left side is the inflow boundary;  $\Gamma_{out}$  on the right side is the outflow boundary; and  $\Gamma_{imp}$  at the top and bottom is the impervious boundary (see Figure 1). There are no source terms inside the domain, and denoting  $\psi^w = \rho_l^w \mathbf{K} \lambda_l \nabla P_l - j_l^h$  and  $\psi^h = \rho_l^h \mathbf{K} \lambda_l \nabla P_l + \rho_g^h \mathbf{K} \lambda_g \nabla P_g + j_l^h$ , the boundary conditions are as follows

- No flux on  $\Gamma_{imp}$

$$(27) \quad \psi^w \cdot \nu = 0 \text{ and } \psi^h \cdot \nu = 0$$

- Injection of hydrogen on the inlet  $\Gamma_{in}$

$$(28) \quad \psi^w \cdot \nu = 0 \text{ and } \psi^h \cdot \nu = 5.57 \times 10^{-6} \text{ kg/m}^2/\text{year}$$

- Fixed liquid saturation and pressure on the outlet

$$(29) \quad P_l = 10^6 \text{ Pa}, \quad S_l = 1, \quad \rho_l^h = 0$$

Initial conditions are uniform throughout the domain, corresponding to a stationary state of saturated liquid and no hydrogen injection,

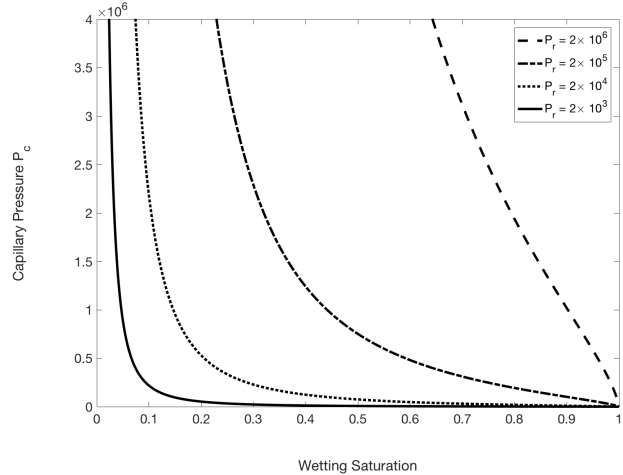
$$(30) \quad P_l = 10^6 \text{ Pa}, \quad S_l = 1, \quad \rho_l^h = 0.$$

The values of the physical parameters are given in Table 1.

Figure 2 shows the Van Genuchten capillary pressure curve for different values of the entry pressure  $P_r$ . These parameter values, along with others in the Van Genuchten model, depend on the porous material. For example, the MoMaS benchmark problem (test case 1 in [10]) uses  $P_r = 2 \cdot 10^6$  for a very dense rock

$K$	$5 \times 10^{-20} m^2$
$\phi$	0.15
$D_l^h$	$3 \times 10^{-9} m^2/s$
$\mu_l$	$1 \times 10^{-9} Pa s$
$\mu_g$	$9 \times 10^{-6} Pa s$
$H$	$7.65 \times 10^{-6} mol/Pa/m^3$
$M^h$	$2 \times 10^{-3} kg/mol$
$M^w$	$1 \times 10^{-2} kg/mol$
$\rho_l^w$	$10^3 kg/m^3$

Table 1: Parameter Values

Fig. 2: Capillary pressure curves for different entry pressure  $P_r$ .

End Time (years)	min		FB		Smooth FB	
	TS	NS	TS	NS	TS	NS
$10^5$	5 (0)	35 (0)	5 (0)	35 (0)	5 (0)	36 (0)
$5 \cdot 10^5$	10 (0)	80 (0)	10 (0)	80 (0)	8 (0)	63 (0)

Table 2: Performance of the nonlinear solver for the capillary pressure model with  $P_r = 2 \times 10^6$  Pa with mesh size of 200.

with extremely low permeability of  $K = 5 \cdot 10^{-20}$ . In other applications including CO<sub>2</sub> sequestration and reservoir simulation, the material is much more permeable and  $P_r = 2 \cdot 10^3$  would produce the capillary pressure curves typically used (see [19, 36]). Other parameters for the Van Genuchten model are  $S_{lr} = 0.4$ ,  $S_{gr} = 0$ , and  $n = 1.49$ . The effect of capillary pressure on the solution is shown in Figure 3, in which the gas saturation throughout the domain is plotted at 100,000 years for  $P_r = 2 \cdot 10^6$  and  $P_r = 2 \cdot 10^3$ . The smaller  $P_r$  is, the steeper the curve becomes near  $S_l = 0$ , and that also makes the problem more difficult to solve. For the MoMaS benchmark case with  $P_r = 2 \cdot 10^6$ , the gas saturation curve exhibits a more gradual transition from the unsaturated to the saturated region. In contrast, for the difficult case of  $P_r = 2 \cdot 10^3$  Pa, the gas saturation changes very quickly both at the injection point and at the interface with the saturated region. We note that the simulation results in Figure 3 match well with those in [23, 32]. A comparison of the performance of the three solution methods is shown in Tables 2 and 3. TS, NS denote the total number of successful time steps and nonlinear iterations, respectively, and the numbers in parentheses are the number of failed time steps and nonlinear iterations. Failed time steps are those in which the method diverges or does not converge within the allowed maximum number of iterations; failed nonlinear iterations correspond to the iterations spent during the failed time steps. For both of these benchmark problems, an initial smoothing parameter  $\tau = 10^{-6}$  and a reduction ratio  $\beta = 0.1$  are used for the smooth Fischer-Burmeister approach.

For the MoMaS gas injection benchmark problem with  $P_r = 2 \cdot 10^6$  Pa, the results in Table 2 show that for the nonlinear solve, the Fischer-Burmeister function (without smoothing) does not show any improvement over the minimum function. It registers the same numbers of time steps needed to run the simulation both to  $10^5$  and to  $5 \cdot 10^5$  years. In contrast, the smooth Fischer-Burmeister function achieves the same performance up to  $T = 10^5$  years, and it reduces both the number of time steps and nonlinear iterations by about 20% for the full simulation. This suggests that the smooth Fischer-Burmeister function is better for simulating long time periods, when the gas phase infiltrates a larger portion of the domain. The second example is exactly the same as the first example, except that we use the entry pressure  $P_r = 2 \cdot 10^3$  for the Van Genuchten

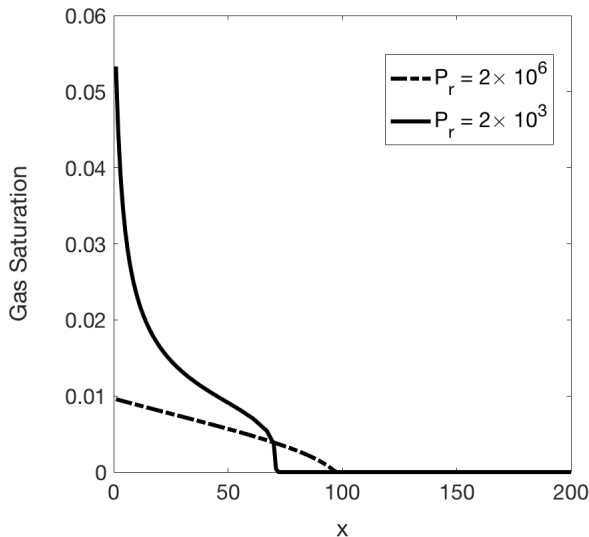


Fig. 3: Gas infiltration into the domain for two different capillary pressure curves after 100,000 years.

Mesh size	min		FB		Smooth FB	
	TS	NS	TS	NS	TS	NS
200	37 (20)	487 (195)	5 (0)	41 (0)	5 (0)	38 (0)
400	59 (48)	949 (440)	6 (0)	59 (0)	5 (0)	42 (0)

Table 3: Performance of the nonlinear solver for the highly nonlinear capillary pressure model with  $P_r = 2 \times 10^3$  Pa after 100,000 years.

model, which makes the problem more difficult to solve. This example illustrates the effectiveness of the smooth Fischer-Burmeister function in handling phase transitions for highly nonlinear problems. We compare the performance of the three different strategies and show the results in Table 3. The semi-smooth Newton method with the minimum function struggles to converge for many time steps. It requires 37 and 59 time steps in total, with 20 and 48 failed time steps for mesh sizes of 200 and 400, respectively. Use of the Fischer-Burmeister function reduces the number of time steps by a factor of seven, and it also requires less than 10% number of nonlinear iterations. This means that on average, we can take about seven times larger time step and achieve approximately 90% decrease in run time with the Fischer-Burmeister function.

The approach using the smooth Fischer-Burmeister function registers about the same number of time steps as the approach using the standard Fischer-Burmeister function and it further decreases the number of time steps by 7% for the mesh size of 200. For the larger mesh of 400, however, the smooth Fischer-Burmeister variant shows a large improvement over the standard Fischer-Burmeister approach, requiring 29% fewer nonlinear iterations.

**5.2. Problems with highly heterogeneous media.** Here, we describe numerical experiments on two problems with highly heterogeneous permeability: (1) a modified two-dimensional SPE-10 problem, and (2) a three-dimensional problem. The permeability fields for these problems are shown in Figures 4a and 4b. In both cases, the entry pressure for the Van Genuchten capillary pressure is chosen as  $P_r = 2 \times 10^3$ , which corresponds to the difficult nonlinear case for the benchmark problem of section 5.1. For the first case, we modify the two-dimensional SPE10 problem [18] by scaling the permeability field by a constant factor of  $10^{-5}$  to make the porous medium more dense. The domain is a rectangle of size  $762m \times 15.24m$ . Pure hydrogen is injected on the left side  $\Gamma_{in} = \{0\} \times [0, 15.24]$ :  $\psi^w \cdot \nu = 0$  and  $\psi^h \cdot \nu = 5.57 \times 10^{-2} kg/m^2/year$ ,

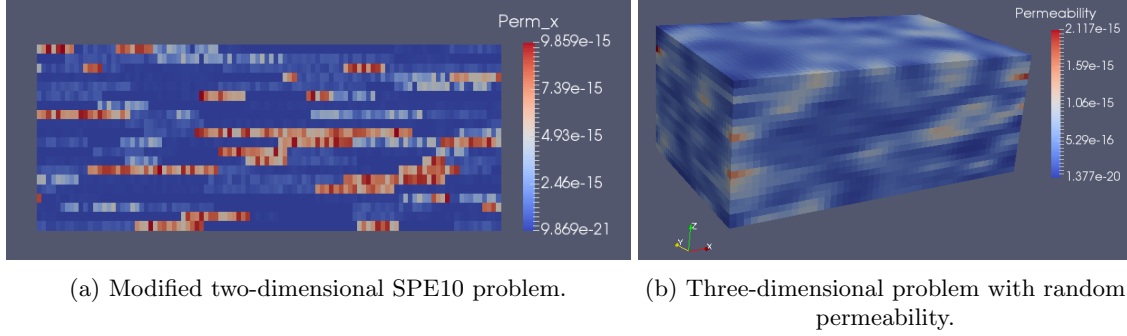


Fig. 4: Heterogeneous Problems.

C-function	Two-dimensional SPE10		Three-dimensional problem	
	FB	Smooth FB	FB	Smooth FB
Number of time steps	60 (7)	37 (4)	13 (4)	8 (3)
Average time step size (days)	19.3	31.3	151.8	250.0
Total nonlinear iterations	856 (147)	530 (84)	202 (84)	135 (63)
Execution time (s)	941.6	566.8	972.6	620.3

Table 4: Performance comparison for heterogeneous problems.

and a Dirichlet boundary condition is given on  $\Gamma_{\text{out}} = \{762\} \times [0, 15.24]$ :  $P_l = 10^6$  Pa,  $S_l = 1$ , and  $\rho_l^h = 0$ . The upper and lower boundary is impervious, i.e.  $\psi^w \cdot \nu = 0$  and  $\psi^h \cdot \nu = 0$ . Initial conditions are  $P_l = 10^6$  Pa,  $S_l = 1$ , and  $\rho_l^h = 0$  for the whole domain. For the spatial discretization, we use a  $100 \times 20$  mesh. The initial time step  $dt = 20$  days and the end time is  $T_{\text{final}} = 1160$  days. The initial smoothing parameter for the smooth Fischer-Burmeister function is  $\tau = 10^{-6}$ .

In the second example, the domain is a box of size  $50m \times 30m \times 20m$ . The porosity and permeability fields are random, generated by a geostatistic model using the open-source code MRST [31]. The porosity has a range of  $[0.002, 0.1]$  and the permeability varies from  $1.377 \cdot 10^{-20}$  to  $2.117 \cdot 10^{-15}$ . Pure hydrogen is injected through the boundary at a corner:  $\psi^w \cdot \nu = 0$  and  $\psi^h \cdot \nu = 5.57 \times 10^{-2} \text{ kg/m}^2/\text{year}$ , and a Dirichlet boundary condition is chosen on the opposite corner:  $P_l = 10^6$  Pa,  $S_l = 1$ , and  $\rho_l^h = 0$ . The rest of the boundary is impervious, i.e.  $\psi^w \cdot \nu = 0$  and  $\psi^h \cdot \nu = 0$ . Initial conditions are  $P_l = 10^6$  Pa,  $S_l = 1$ , and  $\rho_l^h = 0$  for the whole domain. For the spatial discretization, we use a uniform  $50 \times 30 \times 20$  mesh. The initial time step  $dt = 200$  days and the end time is  $T_{\text{final}} = 2000$  days. The initial smoothing parameter for the smooth Fischer-Burmeister function is  $\tau = 10^{-4}$ .

For both of these problems, the semi-smooth Newton approach using the minimum function fails to converge for many time steps, and  $dt$  becomes too small to perform the full simulation. Thus, only the results for the standard Fischer-Burmeister function and the smooth variant are reported in Table 4. Again, the numbers in parentheses are for the failed time steps and nonlinear iterations. The Jacobian smoothing method combined with the smooth Fischer-Burmeister function is more robust than the semi-smooth Newton approach with the standard Fischer-Burmeister function, as demonstrated by the reduction in the number successful and failed time steps. For example, in the two-dimensional SPE10 problem, the former requires only 37 successful time steps and registers 4 failed time steps, as opposed to 60 successful and 7 failed time steps of the latter. In terms of performance, the Jacobian smoothing method combined with the smooth Fischer-Burmeister function is clearly better as it helps decrease the number of nonlinear iterations and execution time by 34-40% approximately for both the two-dimensional and three-dimensional problems.

**5.3. Scaling Results.** To study parallel performance, we use the same setup as for the three-dimensional case with highly heterogeneous media considered in section 5.2. Parallel tests are run on Syrah, a Cray sys-

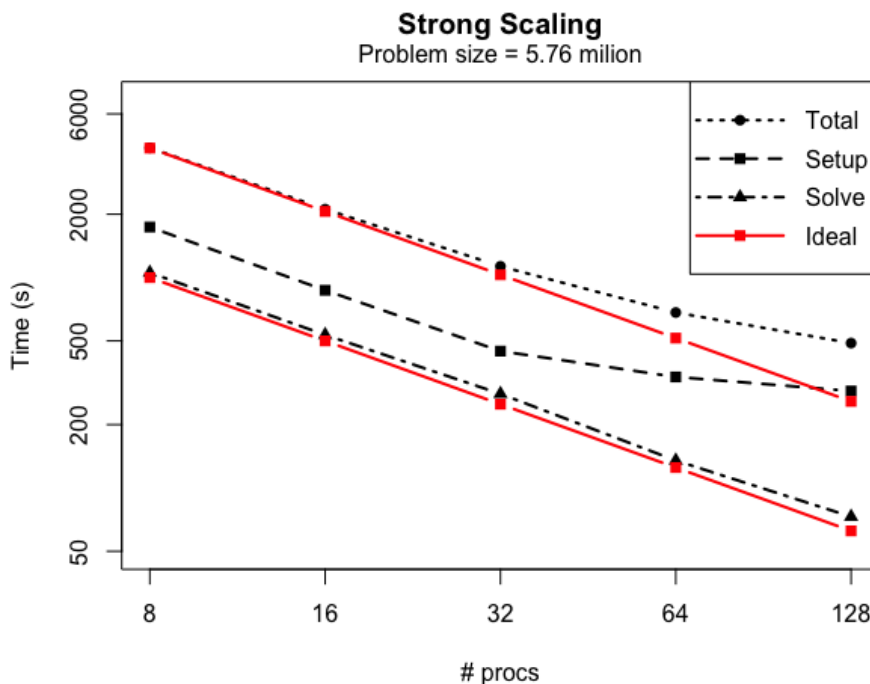


Fig. 5: Strong scaling for the three-dimensional heterogeneous problem. The total runtime for the simulation, the setup, and solve time for the linear solver are reported.

tem with 5,184 Intel Xeon E5-2670 cores at the Lawrence Livermore National Laboratory Computing Center. Amanzi and other libraries are compiled with OpenMPI 1.6.5 and gcc-4.9.2. For strong scaling, the mesh size is fixed at  $200 \times 120 \times 80$ , and the problem has 5.76 million unknowns in total. We choose an initial time step of  $dt = 2$  days and stop the simulation after 20 days. For weak scalability, the number of processors is increased in proportion to the problem size. We use meshes of size  $50 \times 30 \times 20$ ,  $100 \times 60 \times 40$ , and  $200 \times 120 \times 80$  with 2, 16, and 128 processors, respectively. The initial time step is set to  $dt = 2$  days for all the mesh sizes and the simulation is stopped at  $T = 200$  days. For both cases, the entry pressure is set at  $P_r = 2 \times 10^3$ . The results reported in Figure 5 show that the Jacobian smoothing method, combined with GMRES preconditioned by hypreMGR achieves near optimal strong scalability on 8 to 128 processors for the total time needed to run the whole simulation. The slight deviation from the ideal performance at 64 and 128 processors results from the decrease in parallel performance of the setup phase of hypreMGR, which has been observed in [11].

For weak scaling, a comparison between the Jacobian smoothing method using the smooth Fischer-Burmeister function and the semi-smooth Newton approach with the standard Fischer-Burmeister function is shown in Tables 5 and 6. For the semi-smooth Newton method using the standard Fischer-Burmeister function, the simulation does not finish within the 4-hour limit of run time on the cluster. Thus, we only report the solver statistics up to  $T = 38$  days when the simulation terminates. As the mesh is refined, the Jacobian smoothing method is clearly more robust and efficient than the semi-smooth Newton method using the standard Fischer-Burmeister function. Not only does it reduce the number of nonlinear iterations, it also helps improve the performance of the linear solver as indicated by smaller number of linear iterations. The execution time is significantly reduced as a consequence.

**6. Conclusions.** In this work, we have developed a new Jacobian smoothing method based on the smooth Fischer-Burmeister function to solve the discrete nonlinear systems resulting from the fully implicit discretization of the NCP formulation for compositional multiphase flow in porous media with phase transitions. Additionally, we performed various numerical experiments to compare our method with

Number of processors	2	16	128
Mesh size	$50 \times 30 \times 20$	$100 \times 60 \times 40$	$200 \times 120 \times 80$
Initial smoothing parameter $\tau$	$10^{-6}$	$10^{-6}$	$10^{-5}$
Average step size (days)	28.6	28.6	25.0
Number of time steps	7	7	8
Average nonlinear iterations	5.1	6.6	8.9
Average linear iterations	10.7	13.5	17.4
Execution time	122 (s)	286 (s)	995 (s)

Table 5: Weak scaling performance of the Jacobian smoothing method.

Number of processors	2	16	128
Mesh size	$50 \times 30 \times 20$	$100 \times 60 \times 40$	$200 \times 120 \times 80$
Average step size (days)	28.6	25.0	3.45*
Number of time steps	7	8	11 (2)*
Average nonlinear iterations	4.7	6.6	11.1*
Average linear iterations	12.7	22.0	28.5*
Execution time	463 (s)	1623 (s)	> 4 hours

Table 6: Weak scaling performance of the semi-smooth Newton approach using the standard Fischer-Burmeister function.

a semi-smooth Newton approach for two choices of C-function: the minimum and the Fischer-Burmeister functions. The results demonstrate that this method is significantly more robust and efficient with respect to the run time and number of nonlinear iterations. Unlike the semi-smooth Newton method using the minimum function, the Jacobian smoothing approach converges in all examples. Moreover, depending on the problem, it also reduces the number of nonlinear iterations and execution time by 34-40% compared to the semi-smooth Newton method using the standard Fischer-Burmeister function.

## REFERENCES

- [1] A. Abadpour and M. Panfilov. Method of negative saturations for modeling two-phase compositional flow with oversaturated zones. *Transport in Porous Media*, 79(2):197–214, 2008. doi:10.1007/s11242-008-9310-0.
- [2] G. Acs, S. Doleschall, and E. Farkas. General purpose compositional model. *Society of Petroleum Engineers Journal*, 25(04):543–553, 1985. URL: <https://doi.org/10.2118/10515-pa>, doi:10.2118/10515-pa.
- [3] M. Aganagić. Newton’s method for linear complementarity problems. *Mathematical Programming*, 28(3):349–362, 1984. URL: <https://doi.org/10.1007/bf02612339>, doi:10.1007/bf02612339.
- [4] ASCEM. <http://esd.lbl.gov/research/projects/ascem/thrusts/hpc/>, 2009.
- [5] I. Ben Gharbia and J. Ch. Gilbert. Nonconvergence of the plain Newton-min algorithm for linear complementarity problems with a  $P$ -matrix. *Mathematical Programming*, 134:349–364, 2012. URL: <http://dx.doi.org/10.1007/s10107-010-0439-6>.
- [6] I. Ben Gharbia and J. Ch. Gilbert. An algorithmic characterization of  $P$ -matricity. *SIAM Journal on Matrix Analysis and Applications*, 34(3):904–916, 2013. doi:10.1137/120883025.
- [7] I. Ben Gharbia and J.Ch. Gilbert. An algorithmic characterization of  $P$ -matricity II: corrections, refinements, and validation. *SIAM Journal on Matrix Analysis and Applications* (submitted), 2018. [preprint].
- [8] I. Ben Gharbia and J. Jaffré. Gas phase appearance and disappearance as a problem with complementarity constraints. *Mathematics and Computers in Simulation*, 99(0):28 – 36, 2014.
- [9] A. Bourgeat, M. Jurak, and F. Smaï. Two phase partially miscible ow and transport modeling in porous media; application to gas migration in a nuclear waste repository. *Computational Geosciences*, 13(1):29–42, 2008. doi:10.1007/s10596-008-9102-1.
- [10] A. Bourgeat, F. Smaï, and S. Granet. Compositional Two-Phase Flow in Saturated-Unsaturated Porous Media: Benchmarks for Phase Appearance/Disappearance. In *Simulation of Flow in Porous Media*, pages 81–106. De Gruyter, 2013. URL: <http://hal.archives-ouvertes.fr/hal-00965578>.

- [11] Q. M. Bui, L. Wang, and D. Osei-Kuffuor. Algebraic multigrid preconditioners for two-phase flow in porous media with phase transitions. *Advances in Water Resources*, 114:19–28, 2018. doi:10.1016/j.advwatres.2018.01.027.
- [12] B. Chen and P. T. Harker. A non-interior-point continuation method for linear complementarity problems. *SIAM Journal on Matrix Analysis and Applications*, 14(4):1168–1190, 1993. doi:10.1137/0614081.
- [13] X. Chen, Z. Nashed, and L. Qi. Smoothing methods and semismooth methods for nondifferentiable operator equations. *SIAM Journal on Numerical Analysis*, 38(4):1200–1216, jan 2001. doi:10.1137/s0036142999356719.
- [14] X. Chen, L. Qi, and D. Sun. Global and superlinear convergence of the smoothing newton method and its application to general box constrained variational inequalities. *Mathematics of Computation*, 67(222):519–541, apr 1998. doi:10.1090/s0025-5718-98-00932-6.
- [15] X. Chen and Y. Ye. On homotopy-smoothing methods for box-constrained variational inequalities. *SIAM Journal on Control and Optimization*, 37(2):589–616, jan 1999. doi:10.1137/s0363012997315907.
- [16] Z. Chen and R. E. Ewing. Comparison of various formulations of three-phase flow in porous media. *Journal of Computational Physics*, 132(2):362 – 373, 1997. URL: <http://www.sciencedirect.com/science/article/pii/S0021999196956417>, doi:https://doi.org/10.1006/jcph.1996.5641.
- [17] Z. Chen, G. Huan, and Y. Ma. *Computational Methods for Multiphase Flows in Porous Media*. Society for Industrial and Applied Mathematics, 2006. URL: <http://epubs.siam.org/doi/abs/10.1137/1.9780898718942>, arXiv:<http://epubs.siam.org/doi/pdf/10.1137/1.9780898718942>, doi:10.1137/1.9780898718942.
- [18] M. A. Christie and M. J. Blunt. Tenth SPE comparative solution project: A comparison of upscaling techniques. In *SPE Reservoir Simulation Symposium*. Society of Petroleum Engineers (SPE), 2001. URL: <http://dx.doi.org/10.2118/66599-MS>, doi:10.2118/66599-ms.
- [19] H. Class, A. Ebigbo, R. Helmig, H. K. Dahle, J. M. Nordbotten, M. A. Celia, P. Audigane, M. Darcis, J. Ennis-King, Y. Fan, B. Flemisch, S. E. Gasda, M. Jin, S. Krug, D. Labregere, A. N. Beni, R. J. Pawar, A. Sbai, S. G. Thomas, L. Trenty, and L. Wei. A benchmark study on problems related to CO<sub>2</sub> storage in geologic formations. *Computational Geosciences*, 13(4):409–434, 2009. URL: <https://doi.org/10.1007/s10596-009-9146-x>, doi:10.1007/s10596-009-9146-x.
- [20] H. Class and R. Helmig. Numerical simulation of non-isothermal multiphase multicomponent processes in porous media. 2. Applications for the injection of steam and air. *Soil Science Society of America Journal*, 44:892–898, 2002.
- [21] K. H. Coats. An equation of state compositional model. *SPE Journal*, 20(05):363–376, 1980. URL: <https://doi.org/10.2118/8284-pa>, doi:10.2118/8284-pa.
- [22] E. Coon, J. D. Moulton, and S. Painter. Managing complexity in simulations of land surface and near-surface processes. Technical Report LA-UR 14-25386, Applied Mathematics and Plasma Physics Group, Los Alamos National Laboratory, 2014.
- [23] R. De Cuveland. *Two-Phase Compositional Flow Simulation with Persistent Variables*. PhD thesis, University of Heidelberg, 2015. doi:10.11588/heidok.00018629.
- [24] T. De Luca, F. Facchinei, and C. Kanzow. A semismooth equation approach to the solution of nonlinear complementarity problems. *Mathematical Programming*, 75(3):407–439, dec 1996. doi:10.1007/bf02592192.
- [25] F. Facchinei and J. S. Pang. *Finite-Dimensional Variational Inequalities and Complementarity Problems (Springer Series in Operations Research and Financial Engineering)*, volume 2. Springer, 2003.
- [26] P. A. Forsyth, Y-S. Wu, and K. Pruess. Robust numerical methods for saturated-unsaturated flow with dry initial conditions in heterogeneous media. *Advances in Water Resources*, 18(1):25–38, 1995.
- [27] M. Hintermüller, K. Ito, and K. Kunisch. The primal-dual active set strategy as a semismooth Newton method. *SIAM Journal on Optimization*, 13(3):865–888, 2002. URL: <http://dx.doi.org/10.1137/S1052623401383558>, doi:10.1137/S1052623401383558.
- [28] C. Kanzow. Some noninterior continuation methods for linear complementarity problems. *SIAM Journal on Matrix Analysis and Applications*, 17(4):851–868, 1996. doi:10.1137/s0895479894273134.
- [29] C. T. Kelley. Numerical methods for nonlinear equations. *Acta Numerica*, 27:207–287, may 2018. doi:10.1017/s0962492917000113.
- [30] A. Lauser, C. Hager, R. Helmig, and B. Wohlmuth. A new approach for phase transitions in miscible multi-phase flow in porous media. *Advances in Water Resources*, 38:957–966, 2011.
- [31] K. A. Lie, S. Krogstad, I. S. Ligaarden, J. R. Natvig, H. M. Nilsen, and B. Skaflestad. Open-source MATLAB implementation of consistent discretisations on complex grids. *Computational Geosciences*, 16(2):297–322, 2011. URL: <https://doi.org/10.1007/s10596-011-9244-4>, doi:10.1007/s10596-011-9244-4.
- [32] E. Marchand and P. Knabner. Results of the MoMaS benchmark for gas phase appearance and disappearance using generalized MHFE. *Advances in Water Resources*, 73:74 – 96, 2014. URL: <http://www.sciencedirect.com/science/article/pii/S0309170814001390>, doi:https://doi.org/10.1016/j.advwatres.2014.07.005.
- [33] E. Marchand, T. Müller, and P. Knabner. Fully coupled generalised hybrid-mixed finite element approximation of two-phase two-component flow in porous media. Part II: numerical scheme and numerical results. *Computational Geosciences*, 16(3):691–708, 2012. URL: <http://dx.doi.org/10.1007/s10596-012-9279-1>, doi:10.1007/s10596-012-9279-1.
- [34] M. L. Michelsen. The isothermal flash problem. Part II. Phase-split calculation. *Fluid Phase Equilibria*, 9(1):21 – 40, 1982. URL: <http://www.sciencedirect.com/science/article/pii/0378381282850024>, doi:https://doi.org/10.1016/0378-3812(82)85002-4.
- [35] R. Neumann, P. Bastian, and O. Ippisch. Modeling and simulation of two-phase two-component flow with disappearing non-wetting phase. *Computational Geosciences*, 17(1):139–149, 2013. URL: <http://dx.doi.org/10.1007/s10596-012-9321-3>, doi:10.1007/s10596-012-9321-3.
- [36] J. M. Nordbotten, B. Flemisch, S. E. Gasda, H. M. Nilsen, Y. Fan, G. E. Pickup, B. Wiese, M. A. Celia, H. K. Dahle, G. T. Eigestad, and K. Pruess. Uncertainties in practical simulation of CO<sub>2</sub> storage. *International Journal of Greenhouse Gas Control*, 9:234–242, 2012. URL: <https://doi.org/10.1016/j.ijggc.2012.03.007>, doi:10.1016/j.ijggc.2012.03.007.
- [37] L. Qi. Convergence analysis of some algorithms for solving nonsmooth equations. *Mathematics of Operations Research*,

- 18:227–244, 1993.
- [38] L. Qi and J. Sun. A nonsmooth version of Newton’s method. *Mathematical Programming*, 58:353–367, 1993. doi:<http://dx.doi.org/10.1007/BF01581275>.
- [39] Y. Saad and M. H. Schultz. GMRES: A generalized minimal residual algorithm for solving nonsymmetric linear systems. *SIAM Journal on Scientific and Statistical Computing*, 7(3):856–869, 1986. URL: <http://dx.doi.org/10.1137/0907058>, doi:10.1137/0907058.
- [40] M. van Genuchten. A closed form equation for predicting the hydraulic conductivity of unsaturated soils. 25:551–564, 1980.
- [41] Y-S. Wu and P. A. Forsyth. On the selection of primary variables in numerical formulation for modeling multiphase flow in porous media. *Journal of Contaminant Hydrology*, 48:277–304, 2001.
- [42] H. Yang, S. Sun, and C. Yang. Nonlinearly preconditioned semismooth Newton methods for variational inequality solution of two-phase flow in porous media. *Journal of Computational Physics*, 332(Supplement C):1 – 20, 2017. URL: <http://www.sciencedirect.com/science/article/pii/S0021999116306283>, doi:<https://doi.org/10.1016/j.jcp.2016.11.036>.
- [43] L. C. Young and R. E. Stephenson. A generalized compositional approach for reservoir simulation. *SPE Journal*, 23(05):727–742, 1983. URL: <https://doi.org/10.2118/10516-pa>, doi:10.2118/10516-pa.